

# Fast fabrication of microfluidic devices using a low-cost prototyping method

Lei Wang · Wenfang Liu · Shuang Li · Tingting Liu ·  
Xingxing Yan · Yuye Shi · Zeneng Cheng · Chuanpin Chen

Received: 17 December 2014 / Accepted: 5 February 2015 / Published online: 14 February 2015  
© Springer-Verlag Berlin Heidelberg 2015

**Abstract** Conventional ways to produce microfluidic devices cost a lot due to the requirements for cleanroom environments and expensive equipment, which prevents the wider applications of microfluidics in academia and in industry. In this paper, a dry film photoresist was utilized in a simple way to reduce the fabrication cost of microfluidic masters. Thus, a fast prototyping and fabrication of microstructures in polydimethylsiloxane microchips through a replica molding technology was achieved in a low-cost setting within 2.5 h. Subsequently, major manufacturing conditions were optimized to acquire well-resolved microfluidic molds, and the replicated microchips were validated to be of good performance. A T-junction channel microchip was fabricated by using a dry film master to generate water droplets of uniform target size. Meanwhile, a gated injection of fluorescein sodium and a contactless conductivity detection of  $\text{Na}^+$  were both performed in a crosslink channel microchip via capillary electrophoresis, in other words, this fast prototyping and fabrication method would be an efficient, economical way to embody structural design into microfluidic chips for various applications.

## 1 Introduction

There has been an explosion of lab-on-a-chip systems in recent years. Lab-on-a-chip systems offer many advantages such as minimized consumption of samples and reagents, easy integration of sample manipulation, high throughput,

and low cost of analysis (Ansari et al. 2013; Dongre et al. 2010; Zhu and Power 2008). A growing interest in this multidisciplinary field is not only working on individual components fabricated using diverse technologies, but also contributing to the combination of validated fluidic unit operations by identified technologies (Chen and Hahn 2007; Chen et al. 2011; Neuzi et al. 2012).

Polydimethylsiloxane (PDMS) is widely used for the creation of complex microfluidic structures and offers quick fabrication, easy sealing, and biocompatibility (Friend and Yeo 2010; Ibarlucea et al. 2013; Wu and Lee 2012). The microstructures such as channels and pillars are formed in PDMS by casting prepolymer against a master and generating a replica, for example, a ridge on a master appears as a valley in the replica. This process is termed as “replica molding” (Anderson et al. 2000). Prototyping of a microfluidic master is usually achieved by using liquid photoresists or by plasma etching Si wafer by photolithography (Chen et al. 2003; Lin et al. 2002). In particular, SU-8 photoresist was (and is still) the hot technology employed to realize microfluidic microsystem. The conventional methods, however, are complicated and require post-treatments of the master before replica molding. Moreover, the large investment in cleanroom environment and specialized instruments such as spin coaters and ultraviolet (UV) aligners limit the wider applications of microfluidics in academia and in industry.

Dry film photoresists (acrylate-based photopolymers) were originally introduced by Dupont in 1970 for printed circuit board (PCB) fabrication. A dry film photoresist contains a resist layer, sandwiched between a polyester layer, and a polyethylene layer (Reiser 1989). Compared with liquid photoresists, dry film photoresists offer many advantages including uniform photoresist distribution, precise thickness, good conformability, low exposure energy,

---

L. Wang · W. Liu · S. Li · T. Liu · X. Yan · Y. Shi · Z. Cheng ·  
C. Chen (✉)  
School of Pharmaceutical Sciences, Central South University,  
Changsha 410013, Hunan, China  
e-mail: ccpin2000@hotmail.com

short processing time, and excellent adhesion to many substrates such as polyethylene terephthalate (PET). It is now commercially available for various kinds of dry film photoresists, and these films have recently been employed for applications besides the PCB industry, such as in lab-on-a-chip systems (Guijt et al. 2011; Martinez-Duarte 2012). Tsai et al. (2006) fabricated microchannels in dry films through a photolithographic technology to perform microchip capillary electrophoresis (CE). Similarly, dry films were also utilized by Vulto et al. (2005) for fabricating channels to produce hybrid chips. In both prior works, structures of interest were directly etched in dry films to work as microchip modules. However, the prototyping and fabrication process has to be repeated for each chip, which gives rise to low efficiency and high cost. Stephan et al. (2007) accordingly applied dry films to make masters for replications of microchip modules such as channels, reservoirs, and so on. Although the demanded masters were obtained and microchips' performances were also assessed in their applications, an optimized process and a utilization of ordinary instruments were both essential for defining the achievement of fast prototyping and fabrication of microfluidic devices. Additionally, the experimental performances of replicates need to be validated for the various applications of microfluidic chips such as fluid flow control and microchip CE.

In this study, an unconventional method for fast fabrication of PDMS microstructures was developed. It features a non-cleanroom setting, low cost, and simple operation. A commercially available dry film photoresist which can be developed in sodium carbonate solution was utilized to make a rapid and easy fabrication of masters without using any sophisticated instruments. PDMS chips could finally be efficiently obtained with a replica molding technique. Subsequently, the microchips' performances were validated for two important applications. A T-junction microchannel was patterned into a microfluidic chip to generate microdroplets of a given target size. Likewise, a CE on a microchip with two square crosslink channels was also utilized to demonstrate a gated injection of fluorescein sodium and a contactless conductivity detection of  $\text{Na}^+$ .

## 2 Materials and methods

### 2.1 Chemicals and materials

A 25  $\mu\text{m}$  Riston FX-925 dry film (Dupont, USA) was purchased as a negative photoresist for the fast prototyping and fabrication of microfluidic devices, and sodium carbonate solution (Sinopharm Chemical Reagent, China) was selected as the developer solution with a concentration of 0.85 % (w/w). Sylgard 184 (Dow Corning, USA)

prepolymer and its curing agent were thoroughly mixed with a ratio of 10:1 in weight. Deionized water used throughout was prepared by a water purification system (KL-MINI4-T, Kertone, UK). Liquid paraffin (Sinopharm Chemical Reagent, China) with an addition of 3 % span-80 (Tianjin Kemiou Chemical Reagent, China) worked as an oil phase in droplet fabrication. 40 mM fluorescein sodium (Solarbio, China) and 20 mM Tris (Sinopharm Chemical Reagent, China) were respectively selected as a sample and a running buffer in CE for the demonstration of gated injection. MES (Sinopharm Chemical Reagent, China) and His (Aladdin, USA) was mixed with a ratio of 1:1 to work as 10 mM running buffer solution for contactless conductivity detection, and the sample solution was also changed to 1 mM sodium chloride (Sinopharm Chemical Reagent, China) solution. All chemicals were of analytical reagent grade.

### 2.2 Apparatus

The pressing and exposing processes were respectively operated in an office laminator (Simeile, China) and a UV-exposure box (Yongsheng, China). The pattern of photolithographic mask was designed using Adobe Illustrator CS5 (Adobe, USA) and transferred to transparent films as a photomask by a color inkjet printer (iP3600, Canon, Japan). The degassing procedure was performed with a vacuum chamber (Shuniu, China) and a vacuum pump (SHB-III, Xingshuo, China). An oven (101-0AB, Tianjin Taisite Instrument, China) was used for PDMS curing. Syringe pumps (PHD-4400, Harvard Apparatus, USA) were utilized to pump deionized water and liquid paraffin into microfluidic devices. An inverted fluorescence microscope (XDY-2, Chang Sheng Long Apparatus and Meters, China) and a charge-coupled device (CCD) camera (Pixelfly, PCO-TECH, Germany) were used to perform fluorescence imaging. Scanning electron microscopy (SEM) (Quanta 250 FEG, FEI, USA) was utilized to characterize dry film masters. Contactless conductivity detection signal was collected by a home-made contactless conductivity detector.

### 2.3 Prototyping and fabrication of microfluidic devices

Riston FX-925 is a 25- $\mu\text{m}$ -thickness negative dry film photoresist. The general procedure to fabricate dry film masters is illustrated in Fig. 1. Substrates were cleaned ultrasonically in a detergent solution for 10 min, rinsed with deionized water for 10 min, and dehydrated at 80 °C in an oven for 1 h. The photoresist layers were sequentially laminated on the substrate after the protective layer was removed. Multiple layers could be stacked and laminated in the same way to increase the thickness of photoresists.

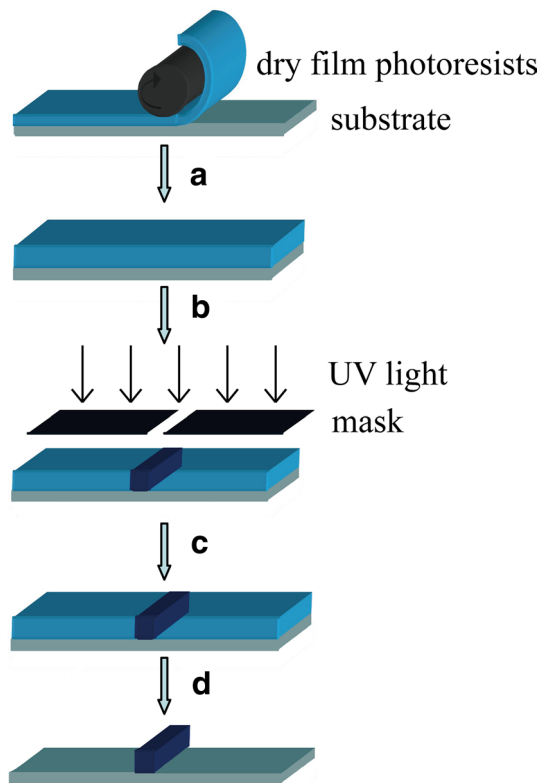


**Fig. 1** Schematic diagram of dry film master fabrication process. To laminate multilayer photoresists on the substrate (a); to expose the photoresists through a photomask with UV irradiation (b); to remove the photolithographic mask and the protective layer on top (c); to develop a final structure in sodium carbonate solution (d)

The photoresists should not have any air bubble and the surface should be flat. The photoresists were then exposed to an irradiation through a photomask in a UV-exposure box, which could prevent undesired exposure effects caused by reflection and non-perfectly parallel exposure. Exposure time was adjusted to the thickness of the layers. After removing the photomask and the protective layer on top, the photoresists were developed by immersing into sodium carbonate solution at 25 °C. The master was then cleaned and dried in an oven for 10 min (Fig. 2). In brief, although some complicated multilayer dry film microstructures, especially 3D structures, might be obtained with a requirement of high-quality aligners and photomasks, which would increase the cost to some extent. However, a commonly used multilayer microstructure in the laboratory could be directly reproduced by repeating aforementioned fabrication steps of laminating, exposing and developing without such specialized instruments and other conventional microfabrication conditions such as cleaning room and spin-coating apparatus.

After a master (Fig. 2a) was designed and fabricated, its quality was verified by SEM (Fig. 2b). Then Sylgard

184 prepolymer and curing agent (10:1) were mixed thoroughly and poured on the master to perform a replication. The mixture, also referred as PDMS, was cured in an oven for 1 h at 60 °C after it was degassed in a vacuum chamber for 30 min. Finally, the replica (Fig. 2c, d) was peeled off by cutting off the polymer around the microstructures and ready for the subsequent applications.

## 2.4 Microfluidic devices setup

### 2.4.1 Microfluidic devices for micro-droplets formation

The experiments were performed in PDMS plate with a T-junction microchannel (Fig. 2c). An channel of 200  $\mu\text{m}$  wide and 100  $\mu\text{m}$  deep in design was for oil flow, and another channel (100  $\mu\text{m}$   $\times$  100  $\mu\text{m}$ ) for water flow was perpendicular to it. A groove worked as a reservoir was set as 2 mm in diameter at the endpoint of each channel. After the microfluidic plate was bonded with another 2-mm-thick PDMS one via corona discharge treatment, the microfluidic chip was finally sealed by curing at 60 °C for 2 h. Then two phases were pumped into the microfluidic device for two-phase flow by two syringe pumps. Deionized water was injected into the main channel, whereas liquid paraffin with 3 % span-80 was injected into the perpendicular channel. All experiments were monitored by a microscope at a magnification of 50  $\times$  and recorded by a CCD camera.

### 2.4.2 Microfluidic devices for microchip CE based on a gated injection mode

In this part, two square crosslink channels were replicated onto a PDMS microchip using above method. As shown in Fig. 3, one channel (a–d) was defined as a separation channel used for sample's separation by CE, and the other one was injection channel (b–c). All the channels were 50  $\mu\text{m}$  in width and 25  $\mu\text{m}$  in depth. After performing a corona discharge on the surfaces, the PDMS microfluidic plate and the substrate were bonded together. Four 2-mm-diameter access holes were drilled at each channel terminal to form reservoirs. The channels were flushed consecutively with ethanol, 0.1 M sodium hydroxide aqueous solution, deionized water, and running buffer (Tris–HCl, 20 mM, pH 7.4) for 15, 30, 30 and 30 min respectively. Then reservoirs (b), (c), and (d) were filled with the running buffer, while reservoir (a) was filled with a sample solution (40 mM fluorescein sodium in buffer). CE was operated with a HV supply and voltage control unit (f). Finally, the assembly was placed on an inverted fluorescence microscope (g) for an observation of the gated injection process.

Subsequently, a contactless conductivity detection of  $\text{Na}^+$  was also performed in the same crosslink microchip with a 100- $\mu\text{m}$ -thickness PET substrate. The microchip

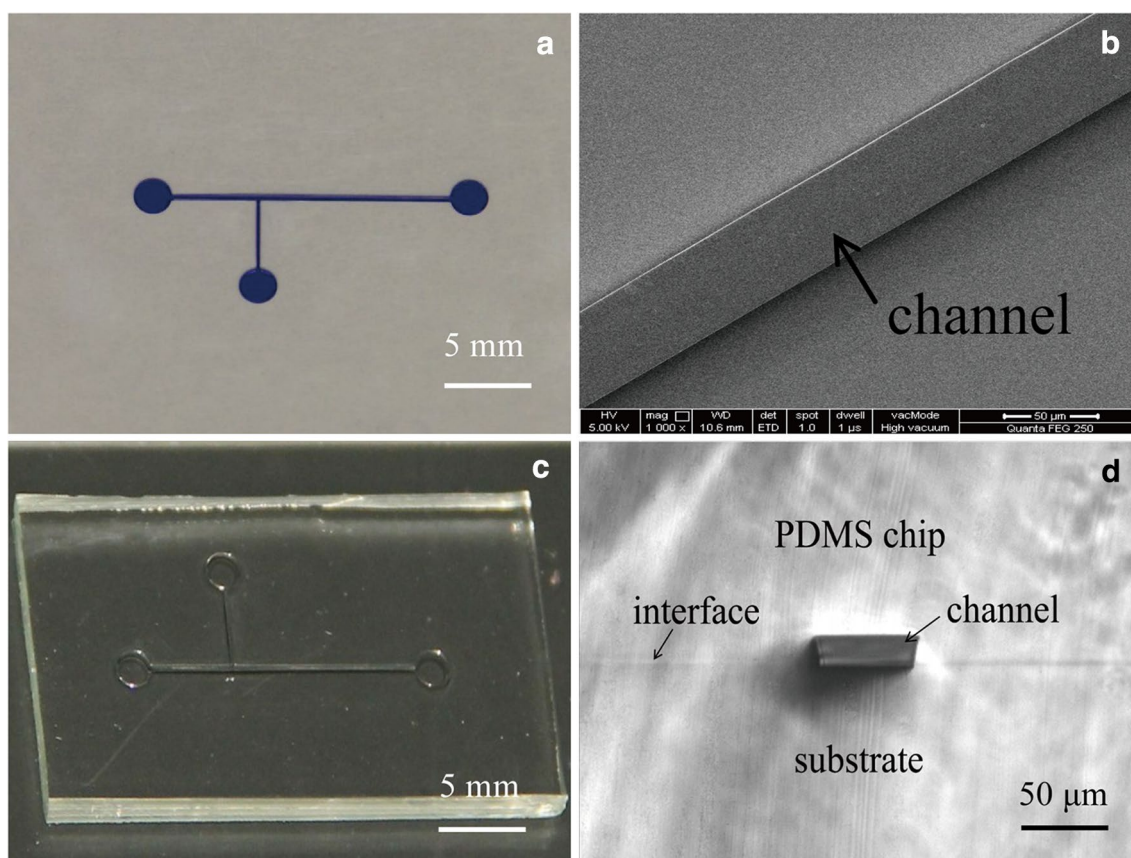


**Fig. 2** A master with a T-junction channel fabricated by using Riston FX-925 dry film photoresists (a), a SEM picture of the dry film master with a straight channel in 50- $\mu\text{m}$  width and 25- $\mu\text{m}$  thickness (b),

a picture of the PDMS microfluidic structure made by a replication of Riston FX-925 master (c), and a micrograph of a cross section of a channel in PDMS substrate (d)

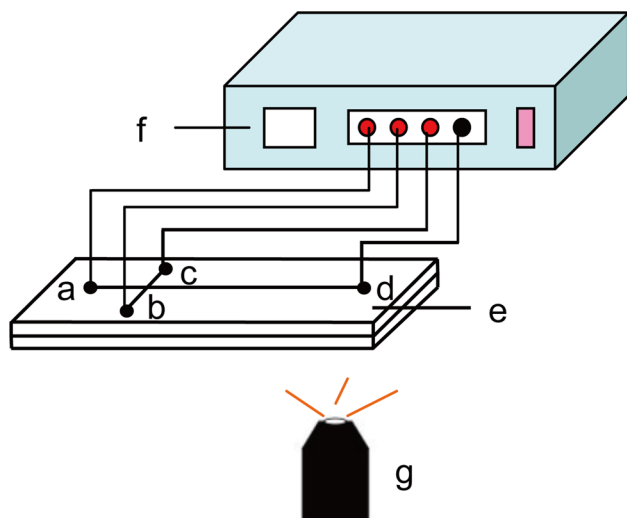


**Fig. 3** Schematic illustration of a gated injection system with a sample reservoir (a), a buffer reservoir (b), a sample waste reservoir (c), and a buffer waste reservoir (d) on a microchip with a pattern of two square crosslink channels (e). The HV supply and voltage control unit (f) was applied for CE operation and the inverted fluorescence microscope (g) was for imaging

was placed on a contactless conductivity detector to make the separation channel pass over the contactless electrodes on the contactless conductivity detector. The length of the two electrodes was 1 mm and the gap between them was 1 mm either. The reservoirs (b), (c), and (d) were filled with a running buffer (MES-His, 10 mM, pH 5.9), and the sample solution in reservoir (a) was changed to 1 mM sodium chloride solution. The sample injection process was going on as aforementioned steps, and contactless conductivity detection signal was collected by the contactless conductivity detector.

### 3 Results and discussion

#### 3.1 Performance and characterization of the photoresist

An optimal substrate is essential for well-resolved microstructures. Various types of substrates, including polymethyl methacrylate (PMMA), glass, PET and PDMS, were evaluated for the fabrication of microstructures. The best results were achieved on PMMA and PET substrates in

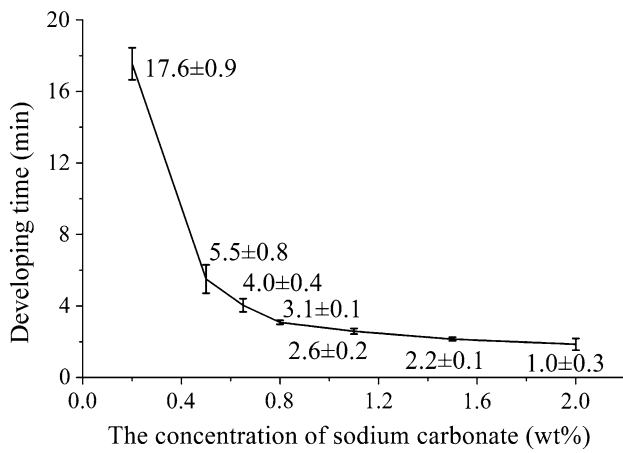


**Fig. 4** Evolution of the developing time with the concentration of the sodium carbonate. Developer’s concentration was ranged from 0.2 to 2 % (w/w). PET was used as a substrate and the results were obtained at 25 °C. The bars represent the optimal time range for each concentration

terms of structure smoothness and bonding strength. There was no damage on the edge of structures, and the dry films were well adhered on the substrates. A weaker adhesion was obtained on the glass substrates, and some structures were deformed as their width decreased. As for the PDMS substrate, photoresist structures just exfoliated completely. Ideally, optimal substrates should contribute to a high resolution as well as a strong adhesion. In this work, PET was chose as the substrate for further research due to its strong adhesion and mechanical strength, good chemical stability, and low cost.

In terms of the developer, sodium carbonate solution rather than organic solvent was used in our work. Compared to organic solvent, sodium carbonate solution was less harmful and required a simple operation process with a low cost. There was a lack of detailed information about the effect of sodium carbonate solution’s concentration on dry film photoresists’ development in reported work (Stephan et al. 2007; Vulto et al. 2005). Therefore, an evolution relationship of developer’s concentration with the

development time required for a well-resolved microstructure in one layer photoresist was obtained to find out an optimal concentration. The photoresist was immersed in sodium carbonate solution for development, and the average time of five repeated experiments in each concentration was obtained at ambient temperature (25 °C). As exhibited in Fig. 4, development time decreased as the sodium carbonate’s concentration increased due to the part of photoresist without a UV irradiation was less stable in higher-concentration developer solution. However, the optimal developer’s concentration was at 0.8–1.1 % (w/w) rather than a higher concentration. For one thing, the development time only reduced little when developer’s concentration increased over 0.8 % (w/w). For high concentration developer, there might be a saturation of dissolved photoresists over the surface of photoresists, and the developing speed is closely related to the diffusion rate of the dissolved photoresists. Thus, a further increase in local concentration of developer could not achieve an acceleration of photoresist’s dissolution. For another, a high concentration of sodium carbonate would cause a rise of solution’s alkalinity, which led to a potential deformation even exfoliation of the photoresist structures. In this case, the developer’s concentration was finally set as 0.85 % in this work.

The dry film photoresists’ thickness was set by controlling the number of the film layers on the substrate. The irradiation time and development time were both varied with photoresists’ thickness for better quality of masters. The evolution relationship of irradiation and development time with photoresists’ thickness was shown in Fig. 5. It exhibited that thicker photoresists required longer irradiation and development. Meanwhile, through visual inspections on the microstructures, it was validated that under-exposure resulted in photoresists’ poor adhesion to the substrate, whereas over-exposure induced an under-etching of the microstructure and so as to a poor resolution. When exposure time was shortened, the amount of light energy radiated on the bottom photoresists would be accordingly reduced because most photons were absorbed by the upper photoresists in the process of exposure. A poor adhesion of

**Fig. 5** Evolution of irradiation time (a) and development time (b) with dry film’s thickness. Dry film photoresists were laminated on the PET substrate and irradiated in a UV-box using a mask patterned a straight channel in 100- $\mu\text{m}$  width and 25- $\mu\text{m}$  thickness

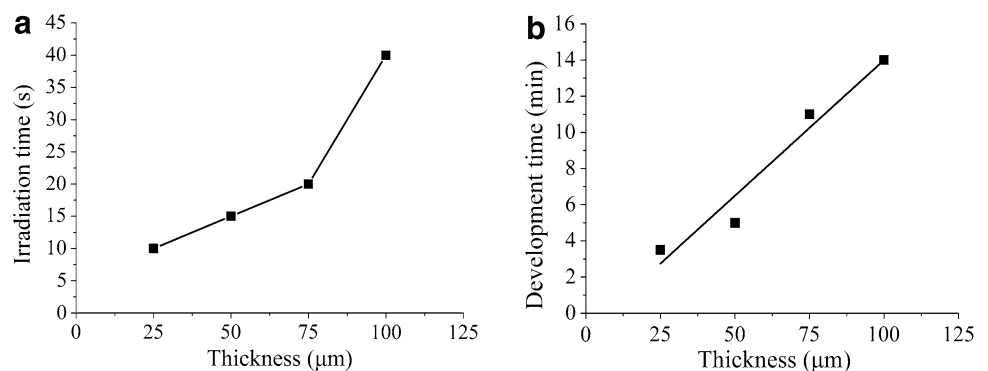


**Table 1** Overview of the setup and consumable cost for fast prototyping and fabrication of microfluidic devices using dry film photoresists in a non-cleanroom setting

Items	Cost
Setup cost	
Red lamp	\$ 5
Office laminator	\$ 30
UV-exposure box	\$ 100
Oven	\$ 250
Vacuum box and pump	\$ 190
Total	\$ 575
Consumables	
Riston FX-925	\$ 0.5/m <sup>2</sup>
Sodium carbonate	\$ 3/kg
Substrates	\$ 90/m <sup>2</sup>
Photolithographic mask	\$ 2.5/A4
Sylgard 184	\$ 160/kg

photoresists to the substrates, even an exfoliation of photoresists, virtually resulted from the insufficient curing of bottom photoresists. On the contrary, a long time exposure would offer a rise of scattering energy, and excessive energy transferred to the bottom. It would accordingly induce a broadening of the curing shape and a poor resolution. Therefore, a proper irradiation time was required for a well-etched microstructure. Due to the design of 100  $\mu\text{m}$  in the height of microstructures for further applications, the optimal irradiation time was set as 40 s.

Accordingly, PET and 0.85 % sodium carbonate solution were selected as the substrate and developer respectively. Under the optimal conditions, the minimum width of 50- $\mu\text{m}$ -thick, 100- $\mu\text{m}$ -thick, and 200- $\mu\text{m}$ -thick photoresists could reach to 50, 50, and 100  $\mu\text{m}$  respectively. As for those applications illustrated in this work, the irradiation time for 100- $\mu\text{m}$ -thick photoresists was set as 40 s, and a minimum width for the microchannel was set as 50  $\mu\text{m}$  under above optimal conditions. PDMS chips were finally achieved with the replicated structures consistent with masters (Fig. 2). Importantly, the size and shape of masters remained the same without a deformation or exfoliation after replicating itself in PDMS for many times (>25).

Dry film photoresists offer many advantages in fast prototyping and fabrication of microfluidic devices, and their greatest contribution is to make those processes accessible to all workers in this field for its low cost and simple process. First of all, the setup cost of this approach could be reduced to \$575 and its consumable cost was also far less than that of other methods as Table 1 showed. Secondly, it took relatively short time (within 2.5 h) to obtain a PDMS chip patterned with a desired structure (Table 2). Lastly, all processes could be undergone in an ordinary setting rather

**Table 2** Overview of the time for fast prototyping and fabrication of microfluidic devices using dry film photoresists in a non-cleanroom setting

Process	Time (min)
Design of photolithographic mask	30–60
Prototyping and fabrication of masks	30–60
Replication	90–120
Total	150–240

than cleanroom environment. That is, it provided an efficient way for researchers to embody their structural designs in chips, and the fabrication of high-quality predesigned microfluidic chips can be achieved as routine work in an ordinary laboratory.

### 3.2 Micro-droplets generation in microfluidics

The microfluidic chip fabricated using the above method was applied to generate micro-droplets. Micro-droplets produced in microfluidic environment have recently been exploited as a novel and exciting platform for chemical and biological sciences. Because of a capacity to mimic conditions similar to that of a single cell, micro-droplets can work as appropriate containers for in vitro biological reactions (Fredlake et al. 2012; Kim et al. 2011; Luo et al. 2006; Minarik et al. 2012). Moreover, through generating and dispersing solution within an immiscible continuous phase, they offer many advantages including an access to ultra-high throughput screen, reduced reagent consumption, improved efficiency through automation, and online analysis as a microreactor for combinatorial chemistry (Li et al. 2010; Osaki et al. 2011; Pei et al. 2010; Wegrzyn et al. 2013; Wu et al. 2011). Channel's performance can impose a great influence on the uniformity of micro-droplets' diameters which are directly related to their properties. One of the most frequently used microfluidic geometries to produce immiscible fluid segments is T-junction channel (Chen et al. 2009; Gunther et al. 2004; Okushima et al. 2004; Srisa-Art et al. 2009). Dry film photoresists in this work were utilized as a master to replicate T-junction channel in PDMS microfluidic chips.

As demonstrated in Fig. 6, water droplets were produced in the T-junction channel in PDMS microfluidic chip. The continuous phase flowed along the main channel, and the discontinuous phase was supplied via the orthogonal inlet. An interface was formed between two immiscible fluids at the junction of the inlet and main channel. The stream of deionized water penetrated into the main channel as the discontinuous phase and a droplet began to grow in the continuous phase (the liquid paraffin with 3 % span-80). The droplet was firstly distorted in the main channel by a

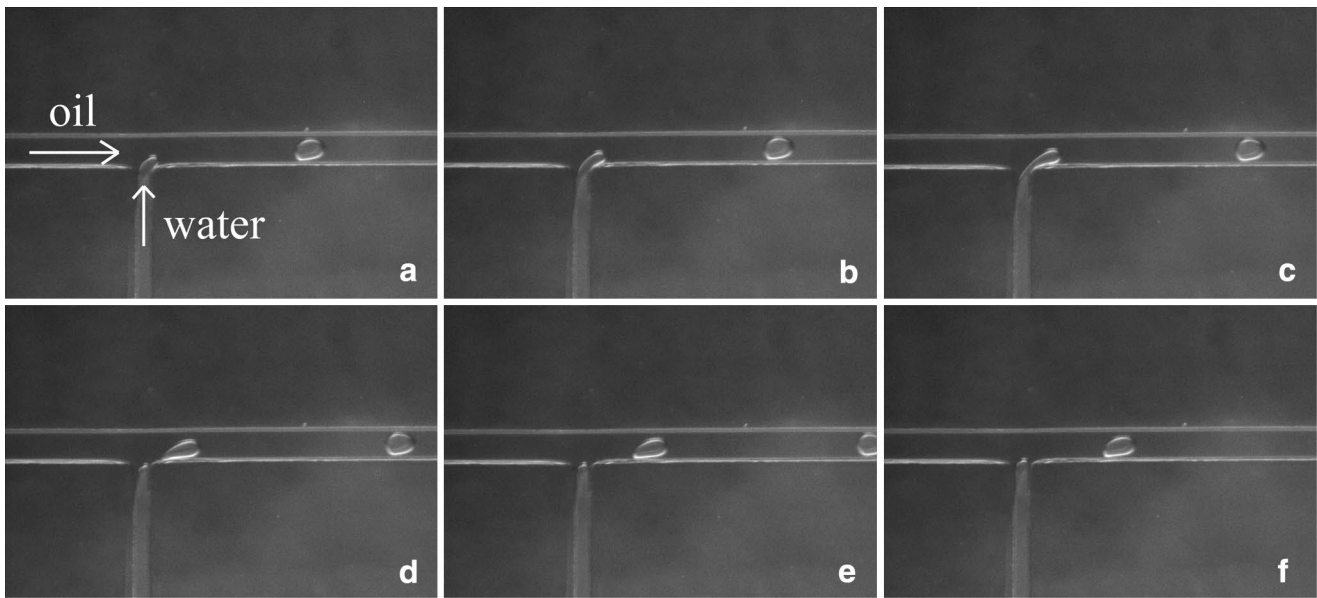
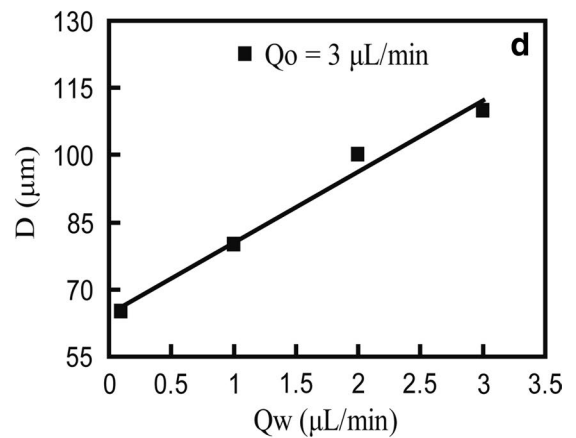
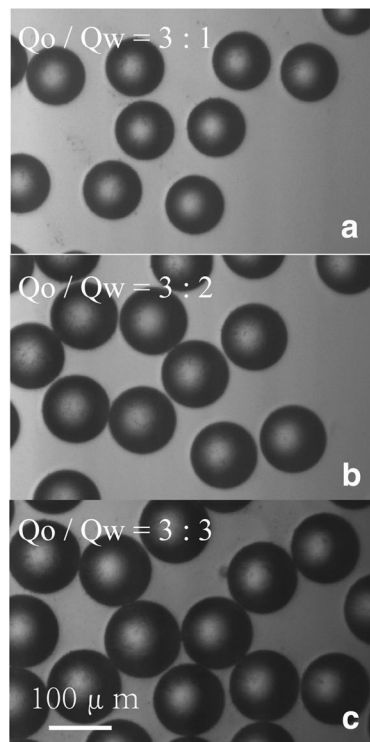


**Fig. 6** Micrographs of the water droplets formation process when an oil phase flow rate was  $3 \mu\text{L min}^{-1}$  and a water phase flow was  $1 \mu\text{L min}^{-1}$ . The recording time interval for the images from (a) to (f) was 0.2 s

**Fig. 7** Micrographs a–c illustrating the influence of water phase flow rate on water droplets’ size at a fixed oil phase flow rate of  $3 \mu\text{L min}^{-1}$ , and an increase in the water phase flow rate at a fixed oil phase flow rate produced larger water droplets (d). The unit of flow rate in the figures is  $\mu\text{L min}^{-1}$



pressure gradient and flowed in the downstream direction, and then the interface on the upstream side of the droplet moved downstream. The neck connecting the inlet channel with the droplet broke until the interface approached the downstream edge of the inlet for the discontinuous phase. The disconnected water plug finally flowed downstream in

the main channel, while the tip of the stream of the deionized water retracted to the end of the inlet and the process repeated.

Droplets in a narrow distribution of individual sizes were achieved in the T-junction channel. Then the effect of two-phase flow rates on droplet’s diameter was investigated. In

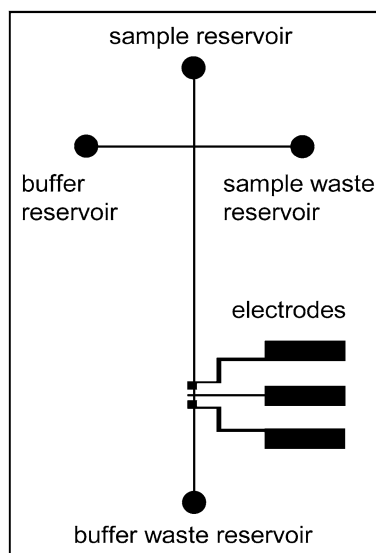


**Fig. 8** Schematic illustration of a microchip used in the microchip CE based on the gated injection mode. The CE microchip was comprised of the top layer and bottom layer. A T-junction microchannel was fabricated on the top layer, and four holes were drilled at the end of all channels to work as sample reservoir, buffer reservoir, sample waste reservoir, and buffer waste reservoir respectively. The ITO electrodes of contactless conductivity detection were integrated on the back of the bottom layer for separating from the T-junction microchannel, and convenient to connect to other additional equipments for contactless conductivity detection

Fig. 7a–c, it clearly noted that the droplets' sizes varied in different water flow rates ( $Q_w$ ) at a fixed oil flow rate ( $Q_o$ ) of  $3 \mu\text{L min}^{-1}$ . Figure 7d illustrated the droplets' diameters increased with water flow rates proportionally. This could lead to applications in precise control of droplets' size in small volumes by changing the flow rate of the dispersed phase.

### 3.3 Application to the microchip CE based on the gated injection mode

Electrokinetic injection is the most widespread method for sample injection in microchip CE (Fu et al. 2002). As one of the electrokinetic injection modes, the gated injection can provide desired volume sample plug, and it is also valuable for repeatable injection with continuous buffer flow (Huang et al. 2008). Since analytes are mainly driven by an electroosmotic flow (EOF) to transport in micro-channel for CE, the injection performance mainly depends on the properties of the micro-channel, especially the cross section of the channel (Tantra et al. 2014; Zhou et al. 2010). Moreover, a well-made micro-channel will contribute to the microchip CE running, thus significantly improving the chip's separation efficiency. Therefore, the microchip CE

based on the gated injection mode can be well performed within a well-fabricated microchip.

In this work, our microchip was utilized to demonstrate the microchip CE based on the gated injection mode (Fig. 8). The gated injection was validated prior to carrying out a contactless conductivity detection of  $\text{Na}^+$  using microchip CE. As shown in Fig. 9a–c, the gated injection was validated by firstly applying 0.7, 1.0, 0.3 kV, and Ground (GND) to the sample reservoir, buffer reservoir, sample waste reservoir, and buffer waste reservoir, respectively. Then, a sample (40 mM fluorescein sodium) plug migrated into the separation channel with EOF by removing the 1.0 kV potential off from the buffer reservoir for 3 s. Finally, the sample injection was completed by reapplying the 1.0 kV potential to the buffer reservoir.

Subsequently, a microchip CE contactless conductivity detection was also demonstrated. The running buffer solution and sample solution were accordingly changed to MES-His solution and 1 mM sodium chloride solution. The gated injection of sample was going on as aforementioned steps, and a signal of  $\text{Na}^+$  was monitored with a migration time of 20 s (Fig. 9d). In a word, the microchips fabricated by replicating dry film photoresist masters in a non-cleanroom setting could exhibit a good performance for CE.

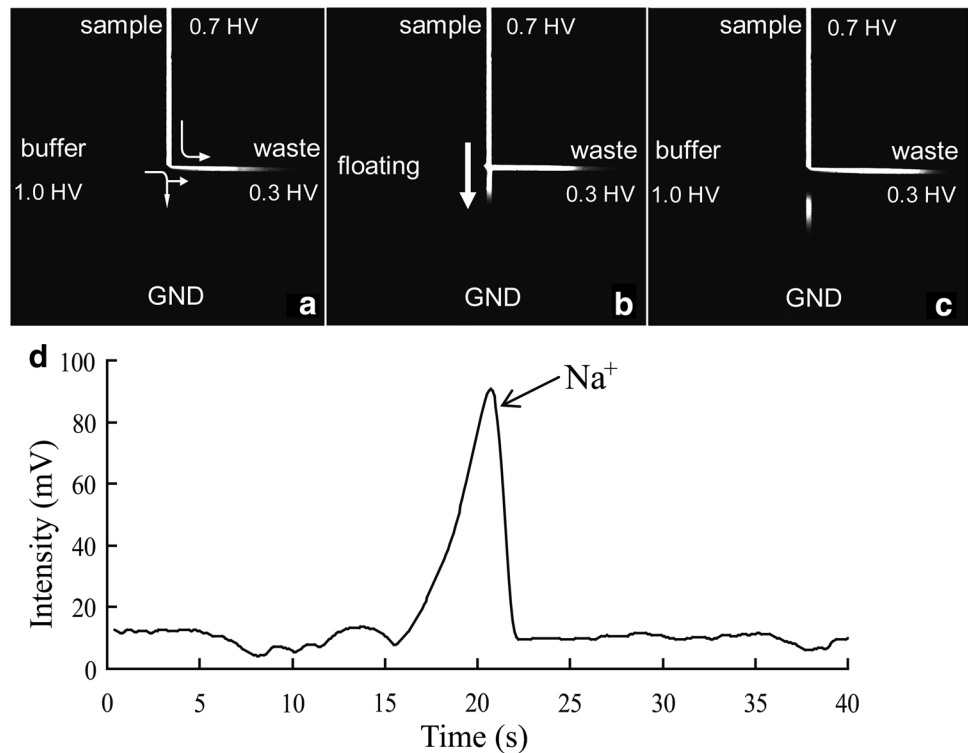
## 4 Conclusion

In this work, a low-cost method was developed for fast prototyping and fabrication of PDMS microstructures, featuring a non-cleanroom setting and simple operation. It also demonstrated that Riston FX-925 dry film photoresists, characterized by their excellent planarity, sensitivity to UV irradiation, and ease of use, could be a suitable alternative to conventional liquid photoresists such as SU-8 for the microfabrication of masters employed to embody desired structural elements into microfluidic chips.

Importantly, not only generation of microdroplets in a T-junction channel, but also gated injection of fluorescein sodium and contactless conductivity detection of  $\text{Na}^+$  using microchip CE were achieved using the PDMS microchips replicated using dry film photoresist masters. The successful applications have proven this material and procedure to be useful for the microfluidic community. In particular, it will enable researchers to routinely conduct the fabrication of high-quality microfluidic chips in an ordinary laboratory for various applications. Moreover, the low cost and simple process of dry film photoresist production will permit the exploiting of other new concepts in the design and fabrication of microfluidic chips for both industrial and research applications in further work.



**Fig. 9** CCD image of the gated injection process including a sample solution ran into the sample waste reservoir when 0.7, 1.0, 0.3 kV, and GND were applied on the sample reservoir, buffer reservoir, sample waste reservoir, and buffer waste reservoir respectively (a); sample plug migrated into the separation channel by floating the buffer reservoir (b); sample solution ran into the sample waste reservoir again, and the sample injection was completed by reapplying 1.0 kV potential on the buffer reservoir (c). All the processes were observed under an inverted fluorescence microscope and recorded by a CCD camera. A contactless conductivity detection signal of  $\text{Na}^+$  appeared within 20 s using the same microchip with the gated injection system (d)



**Acknowledgments** The work was supported by National Natural Science Foundation of China (81202378 and 81311140268). The work also acknowledges the Fundamental Research Funds for the Central Universities of Central South University (7601110178) and the Natural Science Foundation of Hunan Province, China (14JJ4022).

**Conflict of interest** The authors declare that they have no conflict of interest.

## References

- Anderson JR, Chiu DT, Wu H, Schueller OJ, Whitesides GM (2000) Fabrication of microfluidic systems in poly (dimethylsiloxane). *Electrophoresis* 21:27–40
- Ansari K, Ying JYS, Hauser PC, Rooij NF, Rodriguez I (2013) A portable lab-on-a-chip instrument based on MCE with dual top-bottom capacitive coupled contactless conductivity detector in replaceable cell cartridge. *Electrophoresis* 34:1390–1399
- Chen C, Hahn JH (2007) Dual-channel method for interference-free in-channel amperometric detection in microchip capillary electrophoresis. *Anal Chem* 79:7182–7186
- Chen Z, Gao Y, Su R, Li C, Lin J (2003) Fabrication and characterization of poly (methyl methacrylate) microchannels by in situ polymerization with a novel metal template. *Electrophoresis* 24:3246–3252
- Chen C, Zhu Y, Leech PW, Manasseh R (2009) Production of monodispersed micron-sized bubbles at high rates in a microfluidic device. *Appl Phys Lett* 95:144101–144103
- Chen C, Teng W, Hahn JH (2011) Nanoband electrode for high-performance in-channel amperometric detection in dual-channel microchip capillary electrophoresis. *Electrophoresis* 32:838–843
- Dongre C, van Weerd J, Besselink GA, van Weeghel R, Vazquez RM, Osellame R, Cerullo G, Cretich M, Chiari M, Hoekstra HJ (2010) High-resolution electrophoretic separation and integrated-waveguide excitation of fluorescent DNA molecules in a lab on a chip. *Electrophoresis* 31:2584–2588
- Fredlake CP, Hert DG, Niedringhaus TP, Lin JS, Barron AE (2012) Divergent dispersion behavior of ssDNA fragments during microchip electrophoresis in pDMA and LPA entangled polymer networks. *Electrophoresis* 33:1411–1420
- Friend J, Yeo L (2010) Fabrication of microfluidic devices using polydimethylsiloxane. *Biomicrofluidics* 4:26502–26507
- Fu L, Yang R, Lee G, Liu H (2002) Electrokinetic injection techniques in microfluidic chips. *Anal Chem* 74:5084–5091
- Guijt RM, Armstrong JP, Candish E, Lefleur V, Percey WJ, Shabala S, Hauser PC, Breadmore MC (2011) Microfluidic chips for capillary electrophoresis with integrated electrodes for capacitively coupled conductivity detection based on printed circuit board technology. *Sens Actuators B Chem* 159:307–313
- Gunther A, Khan SA, Thalmann M, Trachsel F, Jensen KF (2004) Transport and reaction in microscale segmented gas-liquid flow. *Lab Chip* 4:278–286
- Huang Y, Du W, Pan J, Fang Q (2008) Microfluidic chip-based valveless flow injection analysis system with gravity-driven flows. *Analyst* 133:1237–1241
- Ibarlucea B, Diez-Gil C, Ratera I, Veciana J, Caballero A, Zapata F, Tarraga A, Molina P, Demming S, Buttgenbach S (2013) PDMS based photonic lab-on-a-chip for the selective optical detection of heavy metal ions. *Analyst* 138:839–844
- Kim J, Hwang I, Britain D, Chung TD, Sun Y, Kim D (2011) Microfluidic approaches for gene delivery and gene therapy. *Lab Chip* 11:3941–3948
- Li Q, Pei J, Song P, Kennedy RT (2010) Fraction collection from capillary liquid chromatography and off-line electrospray

- ionization mass spectrometry using oil segmented flow. *Anal Chem* 82:5260–5267
- Lin C, Lee G, Chang B, Chang G (2002) A new fabrication process for ultra-thick microfluidic microstructures utilizing SU-8 photoresist. *J Micromech Microeng* 12:590–597
- Luo C, Yang X, Fu Q, Sun M, Ouyang Q, Chen Y, Ji H (2006) Picoliter-volume aqueous droplets in oil: electrochemical detection and yeast cell electroporation. *Electrophoresis* 27:1977–1983
- Martinez-Duarte R (2012) Microfabrication technologies in dielectrophoresis applications: review. *Electrophoresis* 33:3110–3132
- Minarik M, Kopeckova M, Gassman M, Osmancik P, Benesova L (2012) Rapid testing of clopidogrel resistance by genotyping of CYP2C19 and CYP2C9 polymorphisms using denaturing on-chip capillary electrophoresis. *Electrophoresis* 33:1306–1310
- Neuzi P, Giselsbrecht S, Lange K, Huang TJ, Manz A (2012) Revisiting lab-on-a-chip technology for drug discovery. *Nat Rev Drug Discov* 11:620–632
- Okushima S, Nisisako T, Torii T, Higuchi T (2004) Controlled production of monodisperse double emulsions by two-step droplet breakup in microfluidic devices. *Langmuir* 20:9905–9908
- Osaki T, Yoshizawa S, Kawano R, Sasaki H, Takeuchi S (2011) Lipid-coated microdroplet array for in vitro protein synthesis. *Anal Chem* 83:3186–3191
- Pei J, Li Q, Kennedy RT (2010) Rapid and label-free screening of enzyme inhibitors using segmented flow electrospray ionization mass spectrometry. *J Am Soc Mass Spectr* 21:1107–1113
- Reiser A (1989) *Photoreactive polymers: the science and technology of resists*. Wiley, New York
- Srisa-Art M, Bonzani IC, Williams A, Stevens MM, Edel JB (2009) Identification of rare progenitor cells from human periosteal tissue using droplet microfluidics. *Analyst* 134:2239–2245
- Stephan K, Pittet P, Renaud L, Kleimann P, Morin P, Ouaini N, Ferrigno R (2007) Fast prototyping using a dry film photoresist: microfabrication of soft-lithography masters for microfluidic structures. *J Micromech Microeng* 17:N69–N74
- Tantra R, Robinson K, Sikora A (2014) Variability of microchip capillary electrophoresis with conductivity detection. *Electrophoresis* 35:263–270
- Tsai Y, Jen H, Lin K, Hsieh Y (2006) Fabrication of microfluidic devices using dry film photoresist for microchip capillary electrophoresis. *J Chromatogr A* 1111:267–271
- Vulto P, Glade N, Altomare L, Bablet J, Del Tin L, Medoro G, Chartier I, Manaresi N, Tartagni M, Guerrieri R (2005) Microfluidic channel fabrication in dry film resist for production and prototyping of hybrid chips. *Lab Chip* 5:158–162
- Wegrzyn J, Samborski A, Reissig L, Korczyk PM, Blonski S, Garstecki P (2013) Microfluidic architectures for efficient generation of chemistry gradations in droplets. *Microfluid Nanofluid* 14:235–245
- Wu W, Lee NY (2012) Flow-through PCR on a 3D quadrant-shaped polydimethylsiloxane (PDMS) microdevice employing a single heater: toward microscale multiplex PCR. *Analyst* 137:2069–2076
- Wu N, Courtois F, Surjadi R, Oakeshott J, Peat TS, Easton CJ, Abell C, Zhu Y (2011) Enzyme synthesis and activity assay in microfluidic droplets on a chip. *Eng Life Sci* 11:157–164
- Zhou J, Ellis AV, Voelcker NH (2010) Recent developments in PDMS surface modification for microfluidic devices. *Electrophoresis* 31:2–16
- Zhu Y, Power BE (2008) Lab-on-a-chip in vitro compartmentalization technologies for protein studies. *Adv Biochem Eng Biot* 110:81–114